https://dx.doi.org/10.1016/j.jbiotec.2014.11.004

Biocompatibility, uptake and endocytosis pathways of polystyrene nanoparticles in primary human renal epithelial cells

Daria Maria Monti[1,2], Daniela Guarnieri[3], Giuliana Napolitano[4], Renata Piccoli[1,2], Paolo Netti[3], Sabato Fusco[3], Angela Arciello[1,2]*

[1] Department of Chemical Sciences, University of Naples Federico II, Naples, Italy.

[2] Istituto Nazionale di Biostrutture e Biosistemi (INBB), Rome, Italy.

[3] Center for Advanced Biomaterials for Health Care@CRIB, Istituto Italiano di Tecnologia, and Interdisciplinary Research Centre on Biomaterials, Naples, Italy.

[4] Department of Biology, University of Naples Federico II, Naples, Italy.

*Corresponding author: Angela Arciello, Department of Chemical Sciences, University of Naples Federico II, Complesso Universitario di Monte Sant'Angelo, via Cinthia 4, 80126 Napoli, Italy. Tel: +39–081–679147. Fax: +39–081–679233. E-mail: anarciel@unina.it

Keywords: Polystyrene Nanoparticles – Human Renal Cortical Epithelial Cells – Endocytosis – Nanomedicine

Abbreviations: EIPA, 5-(N-Ethyl-N-isopropyl)amiloride; FITC, fluorescein isothiocyanate; HRCEC, Human Renal Cortical Epithelial Cells; MTT, 3-(4,5-dimethylthiazol-2-yl)-2,5-diphenyltetrazolium bromide; NPs, nanoparticles; PDI, polydispersity index; PS, polystyrene.

https://dx.doi.org/10.1016/j.jbiotec.2014.11.004

ABSTRACT

Recent years have witnessed an unprecedented growth in the number of applications - such as drug delivery, nutraceuticals and production of improved biocompatible materials - in the areas of nanoscience and nanotechnology. Engineered nanoparticles (NPs) are an important tool for the development of quite a few of these applications. Despite intense research activity, mechanisms regulating the uptake of NPs into cells are not completely defined, being the phenomenon dramatically influenced by physico-chemical properties of NPs and cell-specific differences. Since the cellular uptake of NPs is a prerequisite for their use in nanomedicine, the definition of their internalization pathway is crucial. For this reason, we used 44 nm polystyrene NPs as a model to analyse the uptake and endocytosis pathways in primary human renal cortical epithelial (HRCE) cells, which play a key role in the clearance of drugs. NPs were found not to affect the viability and cell cycle progression of HRCE cells. Distinct internalization pathways were analysed by the use of drugs known to inhibit specific endocytosis routes. Analyses, performed by confocal microscopy in combination with quantitative spectrofluorimetric assays, indicated that NPs enter HRCE cells through multiple mechanisms, either energy-dependent (endocytosis) or energy-independent.

https://dx.doi.org/10.1016/j.jbiotec.2014.11.004

1. INTRODUCTION

Nanoparticles (NPs) can be applied in the medical sector as sensors, in cell and organ imaging, implant coatings and drug delivery. Understanding the distinct endocytic mechanism(s) used by NPs to enter the target cell is essential for drug delivery. A thorough and consistent profile of NP uptake is difficult to describe, since literature offers contrasting opinions on this; it has been reported that NPs can enter cells both via passive and active transport and no general rules have been identified so far on size- and surface-dependent particle uptake. Moreover, several endocytic mechanisms often take place simultaneously and the mechanism of internalization may be dramatically influenced by physico-chemical properties (Hillaireau and Couvreur, 2009) of NPs. From a general point of view, a simplified classification of endocytosis into four routes, i.e. clathrin-mediated, caveolae-mediated, macropinocytosis, and caveolae-independent pathways, is generally taken into account (Doherty et al., 2009; Howes et al., 2010; Sahay et al., 2010). Polystyrene (PS) NPs have been widely used as models because they can be easily synthesized in a wide range of sizes, which facilitates their application as biosensors (Velev and Kaler, 1999) in photonics (Rogach et al., 20009) and in self-assembling nanostructures (Boal et al., 2000). It has been reported that positively charged NPs are taken up *via* clathrin-coated vesicles (Jiang et al., 2010), while plain PS NPs mostly use macropinocytosis to enter cells (Jiang et al., 2011). It is noteworthy that differences in the internalization pathways may be due to cell-specific expression of endocytic routes. It is, for instance, known that smooth-muscle cells, fibroblasts, adipocytes and endothelial cells are rich in caveolae (Parton and Simons, 2007) and, therefore, preferentially use the caveolae-dependent route. The purpose of the present work is to analyse uptake, toxicity and stability of 44 nm PS NPs in renal cells. In our study, primary human renal cortical epithelial (HRCE) cells were used, as they play an important role in the clearance of drugs in vivo by reabsorbing glucose and amino acids in the glomerular filtrate, while allowing other substances of no nutritional value to be excreted in the urine. For biomedical applications, nanomaterials need to enter the body and directly contact tissues and cells without any toxic effects; therefore, it is crucial

https://dx.doi.org/10.1016/j.jbiotec.2014.11.004

to explore PS NP biocompatibility. We found that 44 nm PS NPs do not affect viability of HRCE cells and do not interfere with cell cycle progression independently from NP concentration and exposure time. Furthermore, we analysed the internalization pathway(s) of NPs by using different drugs known to inhibit different endocytic pathways. Confocal microscopy analyses, in combination with quantitative spectrofluorimetric assays, allowed us to draw a picture of the uptake mechanisms involved. We demonstrated that 44 nm PS NPs enter HRCE cells through different coexisting mechanisms, either energy-dependent or energy-independent. Our study represents a contribution in defining the internalization pathway of NPs to be used for drug delivery.

https://dx.doi.org/10.1016/j.jbiotec.2014.11.004

2. MATERIALS AND METHODS

2.1. Reagents

Green fluorescent PS NPs with a diameter of 44 nm were purchased from Duke Scientific Corporation (Palo Alto, CA, USA). All reagents and FITC-insulin were from Sigma-Aldrich (St Louis, MO, USA). Mouse anti-human clathrin monoclonal antibody was purchased from ABR Affinity BioReagents (Golden, CO, USA); rabbit anti-human caveolin-1 polyclonal antibodies were from Abcam (Cambridge, UK); fluorescent goat anti-rabbit and anti-mouse IgGs were from Invitrogen (Carlsbad, CA, USA).

2.2. Size and ζ-potential measurements

The particle size and ζ-potential were determined by using a ZetaSizer Nano ZS, Malvern Instruments, Worcestershire, UK. Analyses were performed on NPs diluted in distilled water, serum free cell culture medium and complete cell culture medium. NPs were tested at a concentration of 0.1 mg/mL, following an incubation of 1h at 37°C. All samples were subjected to three measurements and data were reported as mean ± standard deviation (SD).

2.3. Cell culture

Human Renal Cortical Epithelial (HRCE) cells (Innoprot, Derio - Bizkaia, Spain) were cultured in basal medium, supplemented with 2% foetal bovine serum, epithelial cell growth supplement and antibiotics, all from Innoprot, in a 5% CO_2 humidified atmosphere at 37 °C. **2.4. Cell viability and cell cycle analyses**

To test the effects of NPs on cell viability, HRCE cells were seeded in 96-well plates (100 μL/well) at a density of $5x10^3$/well. In the case of long time exposure to NPs (168 h), cells were plated at a lower density ($1x10^3$/well). 24 h after seeding, PS NPs were added to the cells for time- and dose-dependent cytotoxic assays. At the end of incubation, cell viability was assessed by the MTT assay. MTT reagent, dissolved in DMEM in the absence of phenol red, was added to the cells (100 μL/well) to a final concentration of 0.5 mg/mL. Following 4 h incubation at 37 °C, the culture medium was removed and the resulting formazan salts were dissolved by adding isopropanol

containing 0.01 N HCl (100 µL/well). Absorbance values of blue formazan were determined at 570 nm using an automatic plate reader (Microbeta Wallac 1420, Perkin Elmer, Waltham, MA, USA). Cell survival was expressed as a percentage of viable cells in the presence of NPs with respect to control cells grown in the absence of NPs. In all the experiments, controls were performed by supplementing the cell cultures with identical volumes of surfactant for the same lengths of time. For cell cycle analyses, HRCE cells were seeded in 100 mm diameter cell culture dishes at a density of $3x10^4$ cells/mL and incubated at 37 °C with PS NPs at a concentration of 40 µg/mL for 72 or 168 h. Following incubation, cells were detached with non-enzymatic cell dissociation solution, washed with PBS and incubated in ice cold methanol for 20 min at -20 °C. Following incubation, cells were hydrated in PBS for 30 min and centrifuged. Cell pellet was then dissolved in PBS containing 50 µg/mL RNase A. After 30 min at room temperature (RT), cells were centrifuged and dissolved in propidium iodide (PI) staining buffer (0.1% sodium citrate containing 50 µg/mL PI) at a density of $0.5x10^6$ cells/mL. Cell cycle analysis was then performed using a FACS Calibur Flow Cytometer (Becton Dickinson, Oxford, UK). The percentage of cells in each phase of the cell cycle (G1, S and G2/M) was calculated by using Modfit software (Becton Dickinson), and compared with the results obtained with untreated cells as a control.

2.5. Fluorescence studies

HRCE cells were seeded on glass coverslips in 24-well plates and grown to semi-confluency. Cells were incubated for the indicated times in complete medium with green fluorescent PS NPs (10 µg/mL) or FITC-insulin (0.1 mg/mL). In order to inhibit specific internalization pathways, different experimental procedures were used. To inhibit energy-dependent endocytosis, HRCE cells were pre-incubated at 4 °C for 10 min and then incubated with NPs or with FITC-insulin for 1 h at 4 °C. Alternatively, cells were pre-treated with sodium azide (200 µM) for 30 min at 37 °C and then incubated with NPs or with FITC-insulin for 1 h at 37 °C. To inhibit microfilament-mediated endocytosis, cells were pre-treated with lantrunculin A (1 µM) for 10 min at 37 °C and then incubated with NPs for 1 h at 37 °C. To inhibit clathrin-mediated endocytosis, cells were pre-treated

with 900 µM sucrose for 30 min at 37 °C and then co-incubated with NPs or with FITC-insulin for 1 h at 37 °C. Endocytosis mediated by clathrin, caveolin and lipid rafts was inhibited by using dynasore. Cells were pre-treated with dynasore (80 µM) for 30 min at 37 °C and then incubated with NPs for 1 h in the presence of the inhibitor. To inhibit macropinocytosis, cells were pre-treated with ethyl-isopropyl amiloride (EIPA, 100 µM) for 30 min at 37 °C and then incubated with NPs for 1 h in the presence of the inhibitor. At the end of the incubations, cells were treated with 1 µg/mL Hoechst 33342 for 10 min at 37 °C and washed with PBS. Cells were then fixed for 10 min at RT with 2% paraformaldehyde in PBS. For immunofluorescence analyses, cells were permeabilized with 0.5% Triton X-100 in PBS (5 min) and then incubated for 30 min with 3% goat serum in PBS, in order to saturate nonspecific binding sites. Afterwards, cells were incubated overnight at 4 °C with mouse anti-clathrin monoclonal or rabbit anti-human caveolin-1 polyclonal antibodies, and then rinsed with 0.1% Triton X-100 in PBS. Finally, cells were incubated 1 h in the darkness with fluorescent goat anti-rabbit or anti-mouse secondary antibodies. Slides were then washed with 0.1% Triton X-100 in PBS and then with PBS, and mounted in 50% glycerol in PBS. Samples were examined using a Leica 6000 UV microscope and a Leica TCS SP5 confocal microscope, equipped with a Leica application suite software. All images were taken under identical conditions, unless specified differently.

2.6. Spectrofluorimetric analyses

HRCE cells were seeded in 12-well plates and grown to semi-confluency. Cells were then incubated for the indicated times in complete medium containing green fluorescent PS NPs (10 µg/mL), in the presence or absence of specific inhibitors. For NPs releasing experiments, HRCE cells were incubated with NPs for 1 h at 37 °C. The NP medium was then removed and the cells were incubated in fresh medium for different time intervals. At the end of the experiment, cells were lysed in lysis buffer (30 mM Tris, 7M urea, 2M thiourea, 4% chaps). In the following 30 sec incubation, 3 volumes of PBS buffer were added and cell lysates were transferred in 96-well plates.

https://dx.doi.org/10.1016/j.jbiotec.2014.11.004

Samples were then analyzed by automatic plate reader at 488 nm excitation and 505 nm emission wavelengths (Microbeta Wallac 1420, Perkin Elmer, Waltham, MA, USA).

2.7 NP diffusion evaluation

NP diffusion coefficients in cell culture medium at 4°C and 37°C were calculated by using the Stokes-Einstein equation:

$$D = \frac{K_b \cdot T}{3\pi\eta d}$$

where K_b is the Boltzmann constant, T [K] and η are the absolute temperature and the viscosity of the medium, respectively, and d is NP diameter. Viscosity values of cell culture medium at 4 °C and 37 °C were obtained from literature (Safi et al., 2011).

3. RESULTS AND DISCUSSION

3.1. Stability of PS NPs in cell culture medium

The colloidal stability of the 44 nm PS NPs is a crucial parameter in the analysis of cell-nanoparticle interaction (Limbach et al., 2005). Thus, measurements of NP ζ-potential and of the hydrodynamic radius (D_H) in bidistilled water, in serum free cell culture medium and in cell culture

https://dx.doi.org/10.1016/j.jbiotec.2014.11.004

medium supplemented with 2% serum were carried out and are reported in Table 1. We found that, in water, PS NP diameter is 44.53 ± 0.22 nm with a polydispersity index (PDI) of about 0.08 and a ζ-potential of -33.10 ± 1.40 mV. Similar results were obtained in serum free cell culture medium, since nanoparticle size remained almost unvaried with no sign of agglomeration (PDI 0.09), in spite of a modest increase of theζ-potential (Table 1). On the contrary,the presence of serum affected 44 nm NP size inducing an increment of about 100% , with a consequent increase in both PDI and ζ-potential (Table 1). . Our results are in agreement with those reported in the literature, indicating that NP colloidal stability is affected by the presence of serum (Guarnieri et al., 2011; Ehrenberg et al. 2009; Lundqvist et al. 2008; Limbach et al., 2005). Hence, although in our experimental system we used plain and not functionalized PS NPs, NP agglomeration and adsorption of serum proteins on NP surface has to be taken into account Moreover, it has to be noticed that polystyrene density (1.05 g/cm^3) is comparable to that of cell culture medium, thus PS NP sedimentation may be negligible.

3.2. Biocompatibility of PS NPs

The effects of PS NPs on the viability of cultured HRCE cells were then tested. For cytotoxicity assays, cultured cells were incubated with increasing concentrations of NPs (2.5-40 μg/mL) for different lengths of time (24–168 h) at 37 °C. Cell viability was assessed by the MTT reduction assay, as an indicator of metabolically active cells. As shown in Fig. 1a, most of the cells (>90%) treated with NPs were metabolically active. To further analyze the effects of NPs on cell viability, we treated HRCE cells with NPs (40 μg/mL) for 72 h or 168 h, in order to perform cell cycle analyses by flow cytometry. As shown in Fig. 1b, NPs were found not to affect cell cycle progression either after 72 h or after 168 h. Hence, in our experimental system, 44 nm PS NPs were found to be non-toxic.

3.3. PS NP uptake

We tested the ability of HRCE cells to uptake PS NPs. To this purpose, cells were incubated in the presence of green fluorescent NPs at 37 °C for different lengths of time (1–4 h). As shown in Fig. 2,

fluorescent signal associated to NPs was found to be mostly intracellular even after 1 h incubation (Fig. 2a) with overtime accumulation and predominant localization in the perinuclear region after 4 h treatment (Fig. 2b). Internalization was confirmed by quantitative spectrofluorimetric analyses, indicating that a significant NP uptake occurred after 30 min incubation, with a plateau reached after 1 h treatment (Fig. 2c). Renal cortical epithelial cells play a crucial role in renal function, since they reabsorb almost all of the glucose and amino acids in the glomerular filtrate, while allowing other substances of no nutritional value to be excreted in the urine; in view of the above we verified whether NPs, once internalized, are released by the cells. To this purpose, we performed time-course experiments by incubating HRCE cells with 44 nm NPs for 1 h at 37 °C. Following incubation, the NP medium was replaced by fresh medium. The amount of intracellular NPs, measured by spectrofluorimetric analyses at regular time intervals (from 10 to 90 min, Fig. 2d), was found to be unvaried, suggesting that NPs are not released by the cells at least in the experimental conditions tested. Although further studies are needed, this evidence is encouraging, since a reduced NPs clearance may be associated to an increased half-life and a consequent decrease of necessary drug doses. By contrast, an efficient clearance of NPs or their biodegradation into biologically benign components is important to prevent toxic effects, which is crucial for further design and development of biologically targeted nanoparticles for biomedical applications.

3.4. Endocytosis pathways

To learn about the mechanism of NP uptake in HRCE cells, we analysed different routes of endocytosis by using specific inhibitors. Since inhibition of an internalization route often activates other endocytic pathways (Harush-Frenkel et al., 2007; Conner and Schmid, 2003), we operated at the shortest time sufficient to detect NPs intracellularly (1 h) (Fig. 3a). The involvement of energy-dependent endocytosis was analysed using two independent approaches. To this purpose, HRCE cells were either pre-incubated at 4 °C for 10 min, as it is known that cooling a cell culture to 4 °C slows down cellular uptake, or pre-treated with sodium azide (200 μM) for 30 min at 37 °C, as sodium azide is an oxidative phosphorylation inhibitor commonly used to abolish ATP-dependent

https://dx.doi.org/10.1016/j.jbiotec.2014.11.004

processes (Dausend et al., 2008). Following each pre-treatment, cells were incubated with PS NPs for 1 h. Fluorescence microscopy analyses revealed a significant, although partial, reduction of 44 nm NP uptake at 4 °C (Fig. 3b) and in the presence of sodium azide (Fig. 3d)suggesting that NP uptake in HRCE cells is, at least in part, an energy-dependent process. These results are in agreement with those reported in the literature in different experimental systems (Panyam et al., 2002). Moreover, quantitative spectrofluorimetric analyses confirmed the significant reduction of NP uptake in HRCE cells both at 4 °C and in the presence of sodium azide, with 4 °C the most effective condition (Fig. 3c). However, at 4 °C an increase in cell culture medium viscosity and in cell membrane rigidity has to be taken into account. Accordingly, we observed that at 4 °C PS NP diffusion decreased of about 60%, with respect to 37 °C. These observations are in line with previously reported data (Limbach et al., 2005; Safi et al., 2011). Hence, we cannot exclude that the higher decrease in NP uptake upon incubation at 4 °C, with respect to the inhibition obtained in the presence of sodium azide, might depend by these phenomena. As expected, cell treatment with sodium azide is slightly toxic for cells, but it is not responsible *per se* for an increase of cell autofluorescence (Fig. 3c,d). Control experiments, performed by incubating HRCE cells with FITC-insulin (100 µg/mL), revealed a significant inhibition of insulin internalization at 4 °C (Fig. 4b) and in the presence of sodium azide (Fig. 4c). On the basis of this experimental evidence, 44 nm PS NPs appear to enter HRCE cells through different mechanisms, either energy-dependent (endocytosis) or energy-independent, in agreement with previously reported data (Verma et al., 2008). At 4 °C, indeed, mechanisms of endocytic/pinocytic uptake of tracer molecules, such as calcein, are completely blocked (Verma et al., 2008). As expected, in these conditions NP uptake results significantly reduced, even if a consistent fraction of particles still seems to enter cells and to localize into the cytosol. This suggests that, in our experimental conditions, 44 nm PS NPs are also capable of passing through the plasma membrane of cells by direct interaction with the lipid bilayer of cell plasma membrane, as reported by Yacobi et al. (2010).

We then checked whether NP uptake in HRCE cells is mediated by microfilaments. To this purpose, we used latrunculin A, a drug that inhibits actin polymerization, thus interfering with microfilament-mediated processes. HRCE cells were pre-treated with lantrunculin A (1 μM) for 10 min at 37 °C and then incubated with NPs for 1 h at 37 °C. Fluorescence microscopy analyses revealed a significant inhibition of 44 nm NP uptake, with most of the signals remaining close to the cell membrane rather than inside the cell (Fig. 3e). Accordingly, quantitative spectrofluorimetric analyses confirmed a slight but significant effect of lantrunculin A on NP uptake (Fig. 3c). This observation suggests that NP uptake in HRCE cells is, at least in part, a microfilament-mediated process.

Furthermore, we examined the effect of hypertonic sucrose, which has been reported to inhibit endocytosis of receptors, such as LDL receptor and β2-adrenergic receptor, by blocking clathrin-coated pit formation (Heuser and Anderson, 1989). To this purpose, cells were pre-treated with sucrose (900 μM) for 30 min at 37 °C and then incubated with NPs for 1 h at 37 °C in the presence of sucrose, which was found to have a very slight effect on the uptake of PS NPs, as indicated by fluorescence (Fig. 3f) and quantitative spectrofluorimetric (Fig. 3c) analyses. Control experiments, performed by incubating HRCE cells with FITC-insulin (100 μg/mL) for 1 h at 37 °C, revealed a significant inhibition of insulin internalization in HRCE cells in the presence of hypertonic sucrose (Fig. 4d), in agreement with clathrin-mediated internalization of this molecule.

As clathrin plays a major role in the formation of coated vesicles, we analysed the co-localization of NPs with clathrin. HRCE cells were incubated with NPs for 1 h at 37 °C, fixed and immunostained by using anti-clathrin antibodies. As shown in Fig. 5a, no significant co-localization between NPs (green) and clathrin (red) was detectable.

Further experiments were performed to investigate the role of lipid rafts in NP internalization by the use of dynasore, a vital specific inhibitor of dynamin (Macia et al., 2006). Dynamin is known to be involved in clathrin- and caveolin-mediated endocytosis and plays a role in some lipid raft-mediated processes (Kirkham and Parton, 2005); it is a GTP-dependent enzyme that wraps around the neck of

https://dx.doi.org/10.1016/j.jbiotec.2014.11.004

newly formed invaginations on the cell membrane as a coil-like structure to allow the release of the vesicle (Macia et al., 2006). HRCE cells were pre-treated with dynasore (80 μM) for 30 min at 37 °C and then incubated with NPs for 1 h in the presence of the inhibitor. Quantitative spectrofluorimetric analyses (Fig. 3c) indicated a very slight effect of dynasore on theuptake of NPs. To confirm these results, we performed immunofluorescence experiments by using caveolin-1 as a marker. Caveolins are a family of integral membrane proteins representing the principal components of caveolae membranes and are involved in receptor-independent endocytosis. HRCE cells were incubated with NPs for 1 h at 37 °C. Cells were then fixed and incubated with anti-human caveolin-1 antibodies. As shown in Fig. 5b, no significant co-localization of 44 nm NPs (green) with caveolin (red) was observed.

Noteworthy, the size of clathrin-coated vesicles and caveolae was generally reported to range from 50 to 150 nm (Hillaireau and Couvreur, 2009), therefore comparable to 49 and 100 nm NP diameters. Therefore, because of their size, it is unlikely that the PS NPs tested in this study enter cells through the above-mentioned pathways. This observation is in agreement with results reported by Guarnieri et al. (2011), indicating that both 49 and 100 nm PS NPs do not cross cell membrane by clathrin-mediated endocytosis in porcine aortic endothelial (PAE) cells. Indeed, it has been reported that endocytosis of 100 nm poly(lactide-co-glycolide) (PLGA) NPs in primary cultured rabbit conjunctival epithelial cells (RCECs) occurs mostly independently of clathrin- and caveolin-1-mediated pathways (Qaddoumi et al., 2003). Since PS NPs tested in our work have no specific surface functionalization, it is conceivable that they did not enter cells by a receptor-mediated endocytic pathway, but following a different non-specific mechanism. In this direction, a potential alternative mechanism could be macropinocytosis, which is reported to be the preferential route for positively charged PS NPs (Dausend et al., 2008). To analyse the contribution of macropinocytosis in NP internalization, EIPA was used as a specific inhibitor of macropinocytosis, which interfers with the activity of the Na^+/H^+ pump located in membranes (Dausend et al., 2008). HRCE cells were pre-treated with EIPA (100 μM) for 30 min at 37 °C and then incubated with NPs for 1 h in

the presence of the inhibitor. Quantitative spectrofluorimetric analyses (Fig. 3c) indicated that EIPA had a very slight effect on the uptake of 44 nm NPs. However, to interpret these data, problems related to the use of inhibitors have to be taken into account. These include (i) the possibility that more than one route may be inhibited, due to the inhibitor low specificity; (ii) the uptake by compensatory mechanisms when one route is blocked; (iii) the alteration of plasma-membrane proteins; (iv) the disruption of the cortical actin cytoskeleton; and (v) the inhibition of vesicle trafficking (Ivanov, 2008). Hence, although we performed our analyses after the shortest time required to detect NPs in the intracellular compartment (1 h), in order to avoid the activation of alternative endocytic pathways upon inhibition of an internalization route, the question about the role of macropinocytosis can not be unambiguously answered by these studies.

https://dx.doi.org/10.1016/j.jbiotec.2014.11.004

4. CONCLUSIONS

The identification of differences in NP uptake routes between normal and tumor cells is fundamental to develop cytostatic NP-based drugs. Nevertheless, little is known in the literature on the toxicity of NPs and the internalization mechanism in human primary cells. In the present study, we analysed the uptake and release of 44 nm PS NPs by primary human renal epithelial cells as a suitable *in vitro* model. NPs do not exhibit any toxic effect to renal cells, probably due to their inert properties, and they are not released overtime. Therefore, it is conceivable that NPs can be administered at low doses and, upon functionalization with specific biomolecules, can be used to deliver drugs to specific targets and/or subcellular compartments. In addition, the finding that NPs enter cells by different routes opens the way to investigate the role of para/transcellular transport pathways, which represent potential alternative routes for passing through the epithelial cell layer. Indeed, it is possible that NPs use the latter pathways to pass epithelial monolayers by opening the tight junctions, thus offering a new possibility for drug delivery across the blood-brain barrier.

Competing interests

The authors confirm that there are no conflicts of interest.

Acknowledgements

We thank Prof. Riccardo Talevi for helpful discussion. Confocal microscopy investigations were carried out at the CISME (Interdepartmental Centre of Electronic Microscopy) of the University of Naples Federico II. This work was supported by University of Naples Federico II (Programma FARO, Finanziamento per l'Avvio di Ricerche Originali).

https://dx.doi.org/10.1016/j.jbiotec.2014.11.004

REFERENCES

Boal, A. K., Ilhan, F., DeRouchey, J.E., Thurn-Albrecht, T., Russell, T. P., Rotello, V. M., 2000. Self-assembly of nanoparticles into structured spherical and network aggregates. Nature. 404, 746–748.

Conner, S.D., Schmid, S.L., 2003. Nature. Regulated portals of entry into the cell. 422(6927), 37-44.

Dausend, J., Musyanovych, A., Dass, M., Walther, P., Schrezenmeier, H., Landfester, K., Mailänder, V., 2008. Uptake mechanism of oppositely charged fluorescent nanoparticles in HeLa cells. Macromol Biosci. 8(12), 1135-1143.

Doherty, G.J., McMahon, H.T., 2009. Mechanisms of endocytosis. Annu. Rev. Biochem. 78, 857–902.

Ehrenberg MS, Friedman AE, Finkelstein JN, Oberdo¨rster G, McGrath JL (2009) The influence of protein adsorption on nanoparticle association with cultured endothelial cells. Biomaterials 30(4):603–610

Guarnieri, D., Guaccio, A., Fusco, S., Netti, P.A., 2011. Effect of serum proteins on polystyrene nanoparticle uptake and intracellular trafficking in endothelial cells. J. Nanopart. Res. 13, 4295–4309.

Harush-Frenkel, O., Debotton, N., Benita, S., Altschuler, Y., 2007. Targeting of nanoparticles to the chlatrin-mediated endocytic pathway. Biochem. Biophys. Res. Commun. 353(1), 26-32.

Heuser, J.E., Anderson, R.G., 1989. Hypertonic media inhibit receptor-mediated endocytosis by blocking clathrin-coated pit formation. J. Cell Biol. 108(2), 389-400.

Hillaireau, H., Couvreur, P., 2009. Nanocarriers' entry into the cell: relevance to drug delivery. Cell Mol. Life Sci. 66(17), 2873–2896.

Howes, M.T., Mayor, S., Parton, R.G., 2010. Molecules, mechanisms, and cellular roles of clathrin-independent endocytosis. Curr. Opin. Cell Biol. 22(4), 519–527.

Ivanov, A., 2008. Pharmacological inhibition of endocytotic pathways: is it specific enough to be useful? Humana Press, New York.

Jiang, X., Dausend, J., Hafner, M., Musyanovych, A., Röcker, C., Landfester, K., Mailänder, V., Nienhaus, G.U. 2010. Specific effects of surface amines on polystyrene nanoparticles in their interactions with mesenchymal stem cells. Biomacromolecules. 11(3), 748–753.

Jiang, X., Musyanovych, A., Rocker, C., Landfester, K., Mailander, V., Nienhaus, G.U. 2011. Specific effects of surface carboxyl groups on anionic polystyrene particles in their interactions with mesenchymal stem cells. Nanoscale. 3(5), 2028–2035.

Kirkham, M., Parton, R.G., 2005. Clathrin-independent endocytosis: new insights into caveolae and non-caveolar lipid raft carriers. Biochim. Biophys. Acta. 1746(3), 349-63.

Limbach LK, Li Y, Grass RN, Brunner TJ, Hintermann MA, Muller M, Gunther D, Stark WJ (2005) Oxide nanoparticle uptake in human lung fibroblasts: effects of particle size, agglomeration, and diffusion at low concentration. Environ Sci Technol 39(23):9370–9376

Lundqvist M, Stigler J, Elia G, Lynch I, Cedervall T, Dawson KA (2008) Nanoparticle size and surface properties determine the protein corona with possible implications for biological impacts. Proc Natl Acad Sci USA 105(38): 14265

Macia, E., Ehrlich, M., Massol, R., Boucrot, E., Brunner, C., Kirchhausen, T., 2006. Dynasore, a cell-permeable inhibitor of dynamin. Dev. Cell. 10(6), 839-850.

Panyam, J., Zhou, W.Z., Prabha, S., Sahoo, S.K., Labhasetwar, V., 2002. Rapid endo-lysosomal escape of poly(DL-lactide-co-glycolide) nanoparticles: implications for drug and gene delivery. FASEB J. 16(10), 1217-1226.

Parton, R.G., Simons K. 2007. The multiple faces of caveolae. Nat. Rev. Mol. Cell Biol. 8(3), 185–194.

Qaddoumi, M.G., Gukasyan, H.J., Davda, J., Labhasetwar, V., Kim, K.J., Lee, V.H., 2003. Clathrin and caveolin-1 expression in primary pigmented rabbit conjunctival epithelial cells: role in plga nanoparticle endocytosis. Mol. Vis. 9, 559–568.

Rogach, A., Susha, A., Caruso, F., Sukhorukov, G., Kornowski, A., Kershaw, S., Mohwald, H., Eychmuller, A., Weller, H., 2000. Nano- and microengineering: 3-D colloidal photonic crystals prepared from sub-mm-Sized polystyrene latex spheres precoated with luminescent polyelectrolyte/nanocrystal shells. Adv. Mater. 12, 333–337.

M. Safi, J. Courtois, M. Seigneuret, H. Conjeaud, J.-F. Berret The effects of aggregation and protein corona on the cellular internalization of iron oxide nanoparticles. Biomaterials Volume 32, Issue 35, December 2011, Pages 9353–9363.

Sahay, G., Alakhova, D.Y., Kabanov A.V., 2010. Endocytosis of nanomedicines. J. Control Release. 145(3), 182–195.

Sandvig, K., Pust, S., Skotland, T., van Deurs, B., 2011. Clathrin-independent endocytosis: mechanisms and function. Curr. Opin. Cell Biol. 23(4), 413–420.

Velev, O. D., Kaler, E.W., 1999. In situ assembly of colloidal particles into miniaturized biosensors. Langmuir. 15, 3693–3698.

Verma, A., Uzun, O., Hu, Y., Hu, Y., Han, H.S., Watson, N., Chen, S., Irvine, D.J., Stellacci, F., 2008. Surface-structure-regulated cell-membrane penetration by monolayer-protected nanoparticles. Nat. Mater. 7(7), 588–595.

Yacobi, N.R., Malmstadt, N., Fazlollahi, F., DeMaio, L., Marchelletta, R., Hamm-Alvarez, S.F., Borok, Z., Kim, K.J., Crandall E.D., 2010. Mechanisms of alveolar epithelial translocation of a defined population of nanoparticles. Am. J. Respir. Cell Mol. Biol. 42(5), 604–614.

https://dx.doi.org/10.1016/j.jbiotec.2014.11.004

Figure legends

Figure 1. Cell viability and cell cycle analyses upon treatment of HRCE cells with NPs. (**a**) Effects of the treatment of HRCE cells with increasing concentrations of NPs (2.5-40 µg/mL) for different lengths of time (24 – 168 h) at 37 °C. Cell viability was assessed by the MTT assay and expressed as the percentage of MTT reduction with respect to controls (untreated cells). The values are the average of 3 independent experiments carried out with triplicate determinations. (**b**) Cell cycle analyses of HRCE cells treated with PS NPs (40 µg/mL) for 72 or 168 h.

Figure 2. Uptake of green fluorescent PS NPs in HRCE cells. HRCE cells were grown on cover slips, incubated 1 h (**a**) or 4 h (**b**) at 37 °C with PS NPs and analysed by confocal microscopy. Nuclei were stained with Hoechst 3342 (blue). All images were taken under identical conditions. Scale bar 30 µm. (**c**) Quantitative spectrofluorimetric analyses of the uptake ofgreen fluorescent PS NPs in HRCE cells. (**d**) Quantitative spectrofluorimetric analyses of the release of PS NPs by HRCE cells.

Figure 3. Analysis of endocytosis pathway of 44 nm PS NPs. HRCE cells were pre-incubated at 4 °C for 10 min (**b**), pre-treated with 200 µM sodium azide for 30 min at 37 °C (**d**), 1 µM lantrunculin A for 10 min at 37 °C (**e**) or 900 µM sucrose for 30 min at 37 °C (**f**). Following pre-treatment, cells were incubated with NPs for 1 h at 37 °C. Untreated HRCE cells are shown in (**a**). Cells were analysed by epifluorescence microscopy. Scale bar 30 µm. (**c**) Quantitative spectrofluorimetric analyses of the effects of different drugs and experimental conditions on the uptake of green fluorescent PS NPs in HRCE cells.

Figure 4. Analysis of FITC-insulin endocytosis in HRCE cells. Cells were pre-incubated at 4 °C for 10 min (**b**), pre-treated with 200 µM sodium azide for 30 min at 37 °C (**c**), or with 900 µM sucrose for 30 min at 37 °C (**d**). Following pre-treatment, cells were incubated with FITC-insulin for 1 h at 37 °C. Untreated HRCE cells are shown in (**a**). Cells were analysed by epifluorescence microscopy. Scale bar 30 µm.

https://dx.doi.org/10.1016/j.jbiotec.2014.11.004

Figure 5. Endocytosis of 44 nm NPs in HRCE cells. Cells were grown on cover slips, incubated with NPs (green) for 1 h at 37 °C and immunofluorescently stained for clathrin (**a**, red) or caveolin-1 (**b**, red). Nuclei were stained with Hoechst 3342 (blue). Cells were analysed by confocal microscopy. Scale bar 30 µm.

Table 1. Size, polydispersity index and zeta-potential of PS NPs in different experimental conditions. Data are reported as mean value ± SD (n=3).

https://dx.doi.org/10.1016/j.jbiotec.2014.11.004

Figure 1.

a

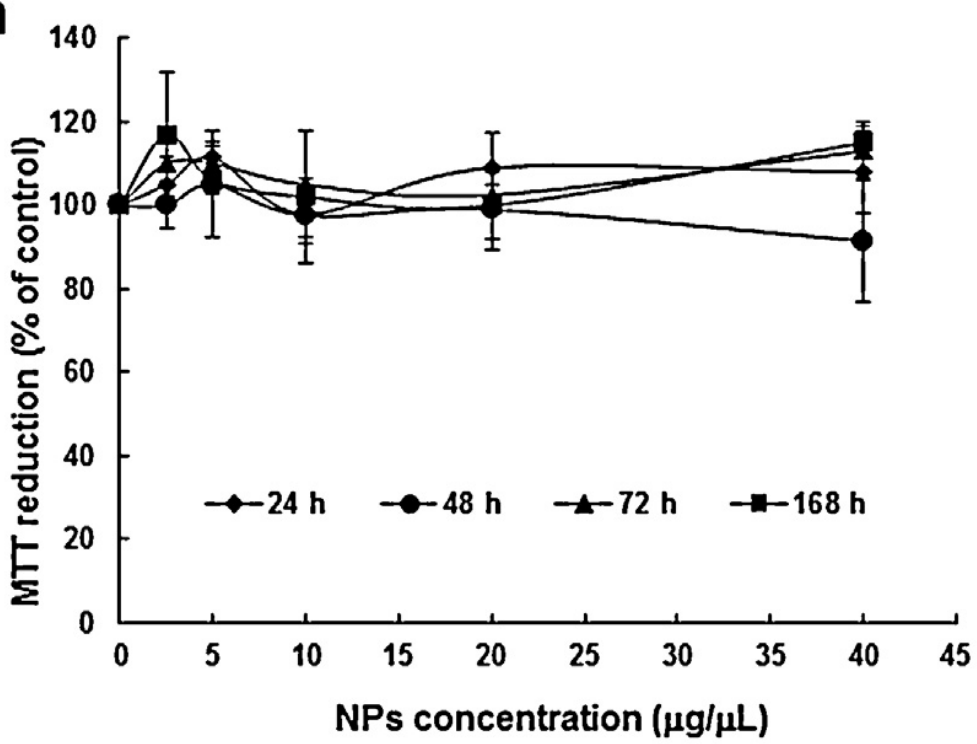

b

	G0/G1 (% cells)	S (%cells)	G2/M (% cells)
Control	80.75±8.49	11.37±1.37	7.88±0.94
NPs 40 μg/μL 72 h	76.30±7.53	9.96±0.58	13.74±1.86
NPs 40 μg/μL 168 h	79.36±5.78	10.85±1.79	9.79±1.59

https://dx.doi.org/10.1016/j.jbiotec.2014.11.004

Figure 2.

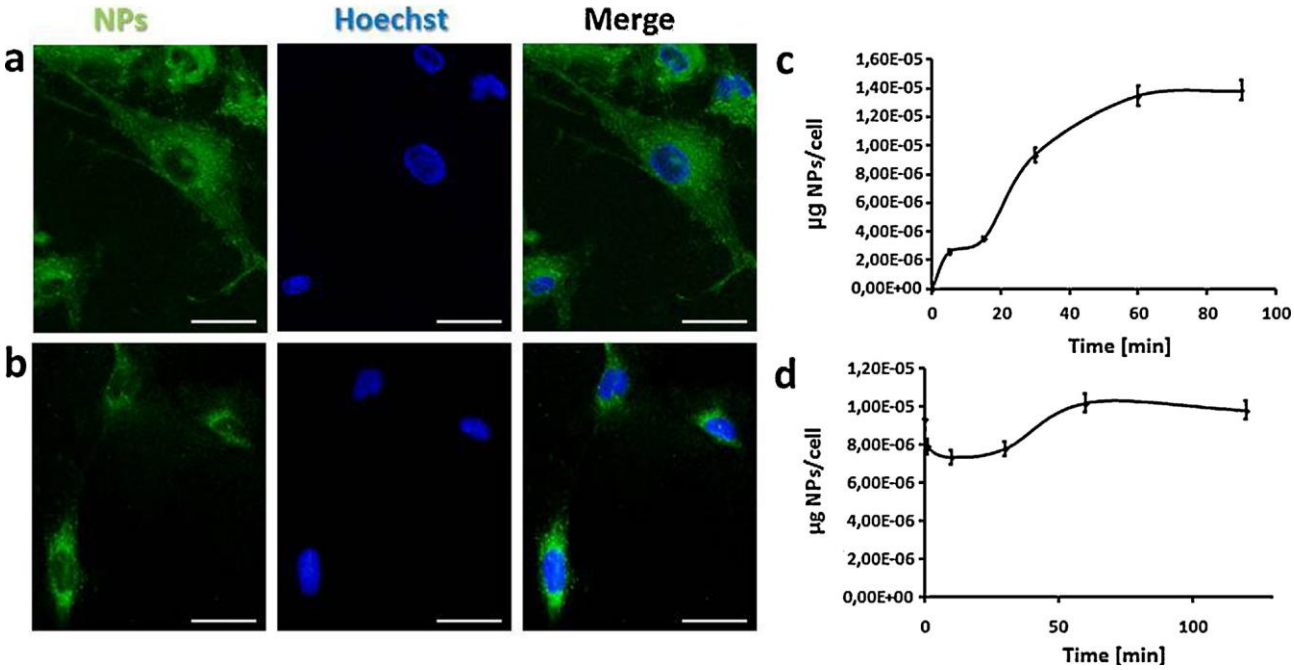

https://dx.doi.org/10.1016/j.jbiotec.2014.11.004

Figure 3.

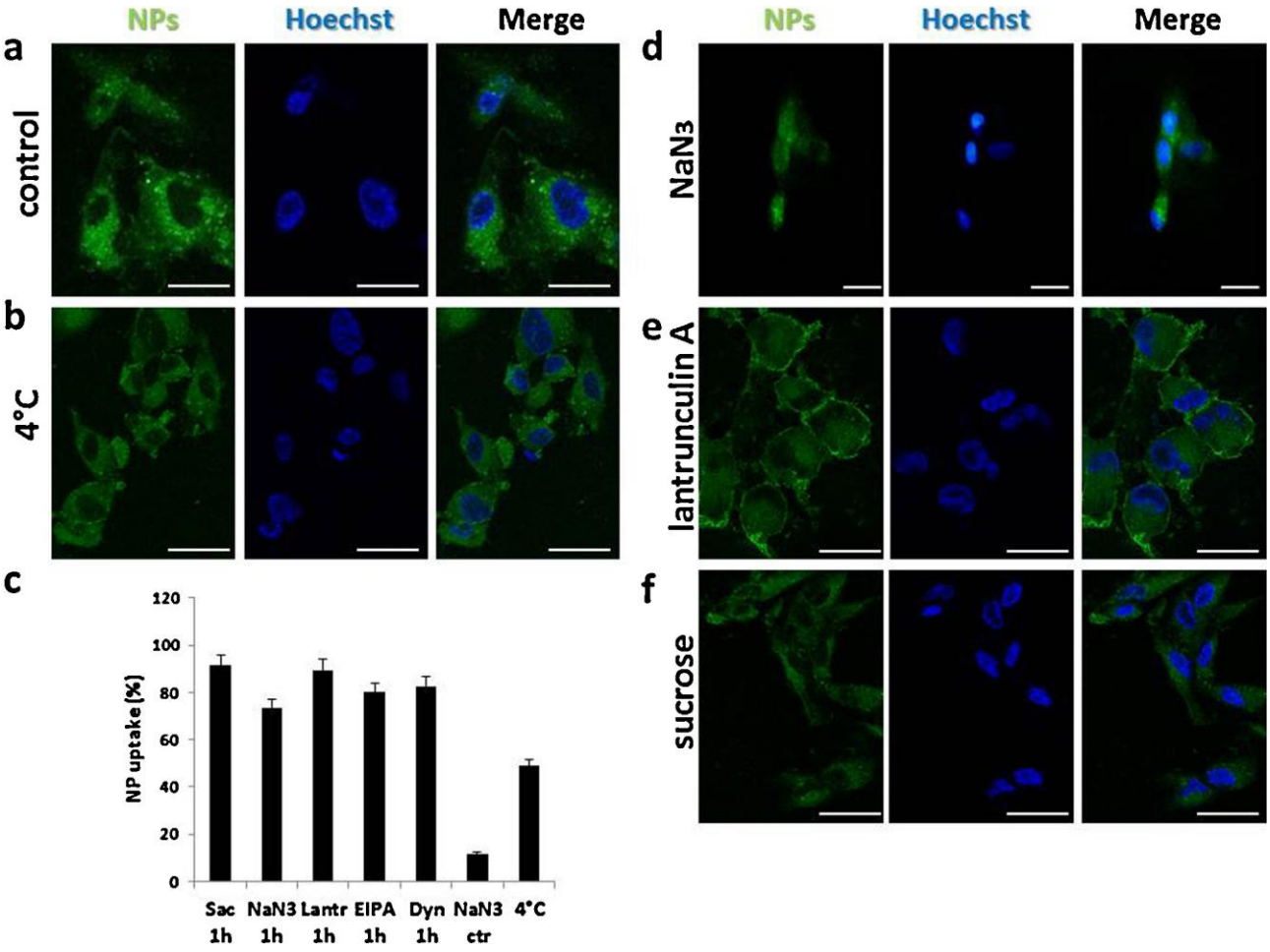

https://dx.doi.org/10.1016/j.jbiotec.2014.11.004

Figure 4.

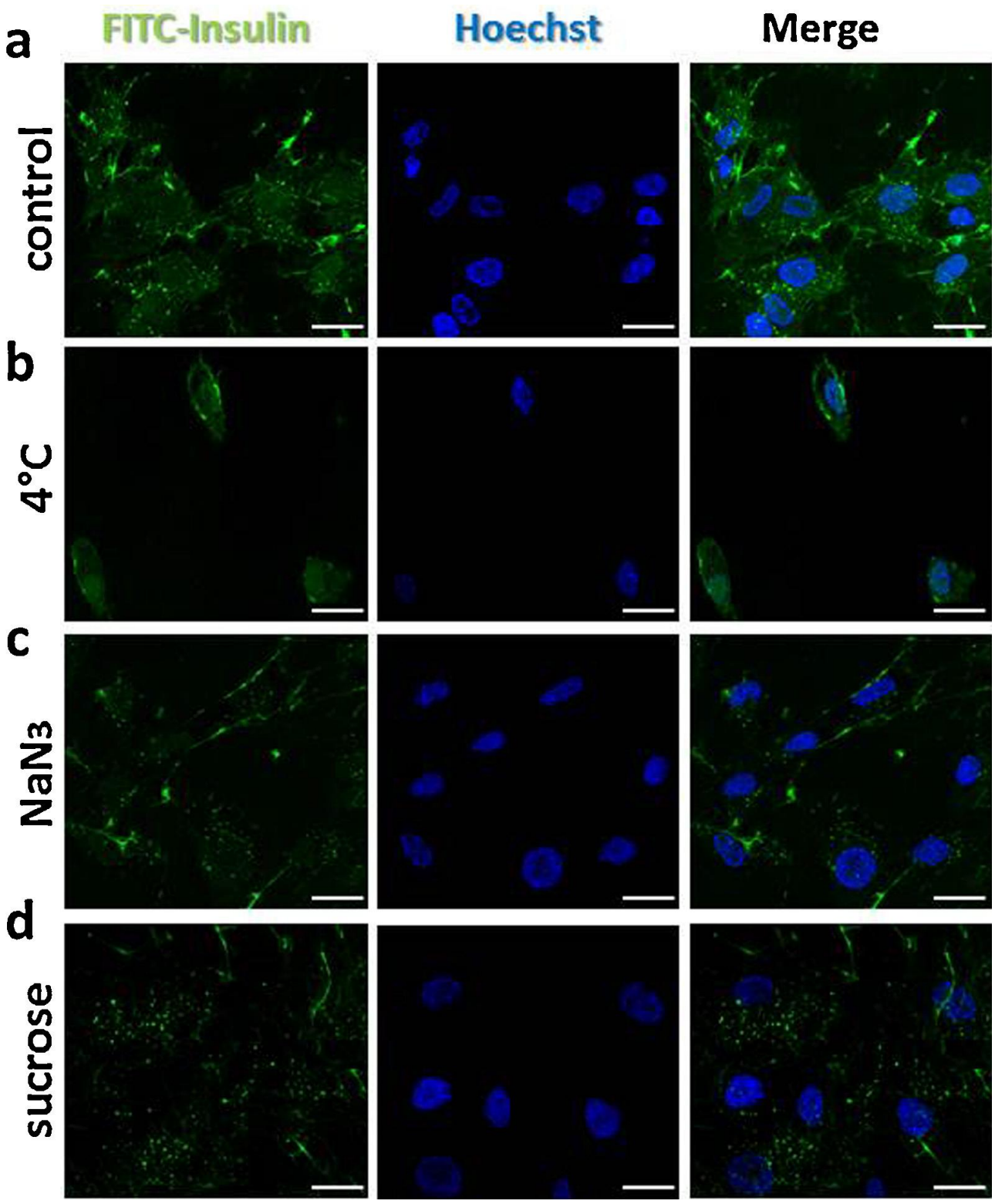

https://dx.doi.org/10.1016/j.jbiotec.2014.11.004

Figure 5.

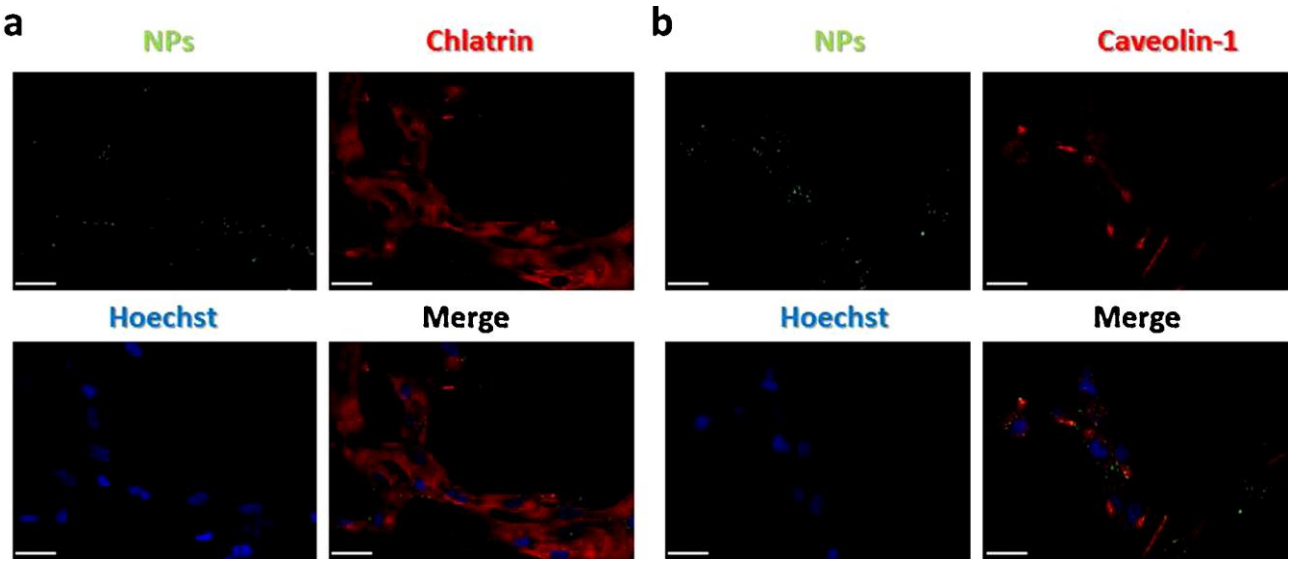

https://dx.doi.org/10.1016/j.jbiotec.2014.11.004

Table 1.

	Size (NP diameter, nm)	PDI	Zeta-potential (mV)
H2O	44.53 ± 0.22	0.08	-33.10 ± 1.40
Serum free medium	42.89 ± 0.43	0.09	-24.6 ± 1.11
Complete cell culture medium	98.23 ± 0.82	0.28	-9.83 ± 0.73